Jonathan Chambers[1], Philip Meldrum[1], David Gunn[1] , Paul Wilkinson[1], Andrew Merritt[1,2] , William Murphy[2], Jared West[2] , Oliver Kuras[1], Edward Haslam[1] , Peter Hobbs[1], Catherine Pennington[1] , Chris Munro[1]

Geophysical-geotechnical sensor networks for landslide monitoring

(1) British Geological Survey, Geophysical Tomography, Nottingham, NG12 5GG, United Kingdom (Jonathan.Chambers@bgs.ac.uk)

(2) University of Leeds, School of Earth and Environment, Leeds, LS2 9JT, United Kingdom

Abstract In this study we describe the development of an integrated geophysical/geotechnical sensor network for monitoring an active inland landslide near Malton, North Yorkshire, UK. The network is based around an automated time-lapse electrical resistivity tomography (ALERT) monitoring system, which has been expanded to incorporate geotechnical sensor arrays. The system can be interrogated remotely using wireless telemetry to enable the near-real-time measurement of geoelectric, geotechnical and hydrologic properties.

The overarching objective of the research is to develop a 4D landslide monitoring system that can characterise the subsurface structure of the landslide, detect changes in the slope, and reveal the hydraulic precursors to movement. Results to-date have shown that ALERT can characterise 3D landslide features, and detect changes associated with seasonal temperature and subsurface moisture content changes, and crucially, the displacement of geophysical sensor arrays that allows the motion of the landslide to be monitored in near-real-time.

Keywords electrical resistivity tomography (ERT), sensor-network, wireless, telemetry, monitoring

Introduction

Geoelectrical ground imaging techniques, such as electrical resistivity tomography (ERT) and self-potential are being increasingly applied to study landslide structure and the processes associated with slope failure (Jongmans and Garambois, 2007). The great strengths of these techniques are that they provide spatial or volumetric subsurface information at the site scale, which, when calibrated with appropriate geotechnical and hydrogeological data, have the potential to characterise lithological variability and monitor hydraulic changes associated with failure events (Lebourg et al., 2005). Here we describe the development and application of an integrated geoelectrical and geotechnical monitoring network on an active landslide in the UK, with the aim of developing new investigative and predictive tools for slope assessment.

Site Description

The research site is located near Malton, North Yorkshire, UK, on a south facing valley side with a slope of approximately 12 degrees (Figure 1). The bedrock geology (Ford, in press), from the base to top of slope, comprises the Lias Group Redcar Mudstone Formation (RMF), Staithes Sandstone and Cleveland Ironstone Formation (SSF), and Whitby Mudstone Formation (WMF), which are overlain at the top of the hill by the Dogger Formation (DF). The bedrock is relatively flat lying with a gentle dip to the north. Slope failure at the site is occurring in the weathered WMF, which is highly prone to landsliding.

The landslide is characterized by shallow rotational failures at the top of the slope that feed into larger-scale slowly moving lobes of slumped material; the rotational features and active lobes extend approximately 150 m down the slope from the top of the hill, and extend laterally more than 1 km along the valley side. In recent years, movement of the lobes has been in the order of tens of centimetres per annum. Movement typically occurs in the winter months (i.e. January and February) when the slope is at its wettest. During this period water can be observed accumulating in the sag ponds caused by rotational slips towards the top of the slope, and can be seen emerging from the front of the lobes. Drainage from the site also occurs along a spring line at the base of the SSF, where groundwater runs off the surface of the less permeable underlying RMF. Piezometers installed at the site have revealed elevated pore pressures at the failure planes within the slipped WMF and at the interface between the slipped WMF material and the underlying SSF.
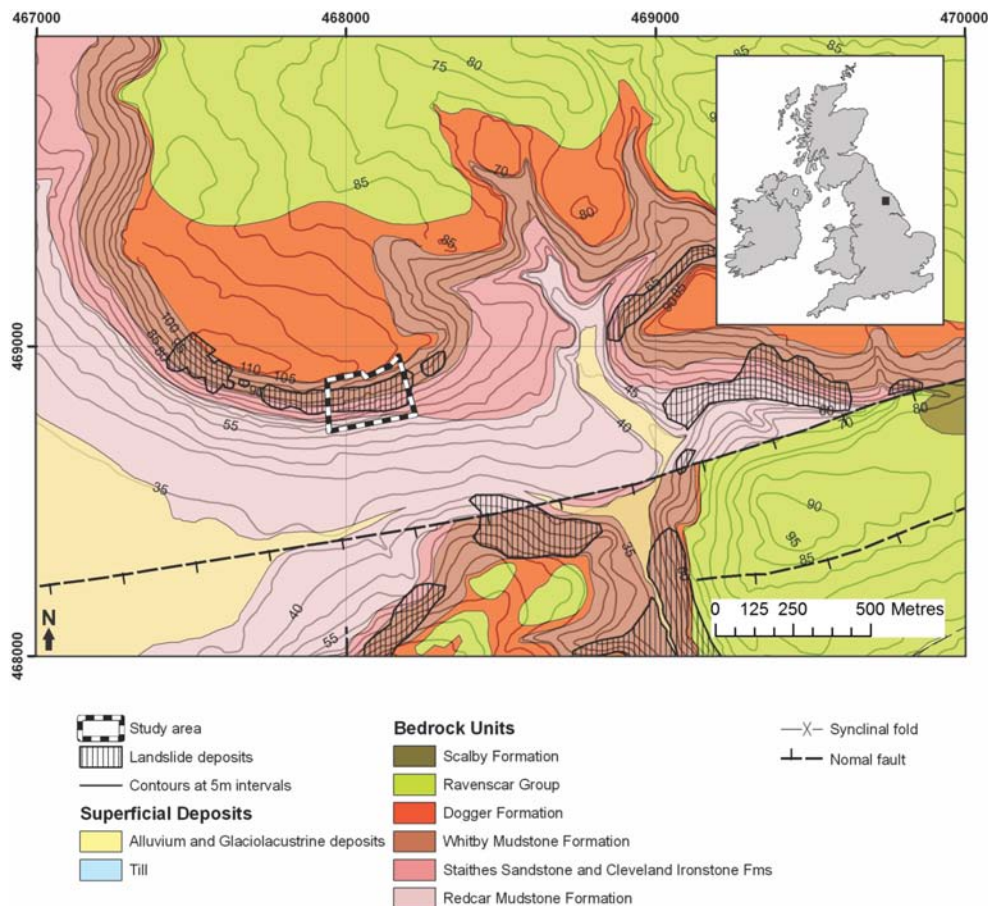
Figure 1 Geological map based on the geological resurvey of the area, showing the location of the study site and the distribution of landslide deposits. Coordinate systems are given as British National Grid (bold) and latitude and longitude (normal). Inset map (top right) shows the location of the study site within the UK.

Methodology

Monitoring instrumentation (ALERT)

Monitoring at the site is based around the ALERT (Automated time-Lapse Electrical Resistivity Tomography) survey concept (Kuras et al., 2009; Ogilvy et al., 2009; Wilkinson et al., 2010a). The ALERT system provides the full capability for remote measurement, storage and transmission of geoelectrical data. It has been designed as a single case unit that can be deployed at a remote location. Once set up at a monitoring site, the system is designed to operate autonomously (Figure 2). It comprises several intelligent sub-systems that co-ordinate and control all the major functions: data collection, data storage, data transmission (to a remote host PC) and handling of data and control scheduling issues. The system is remotely configurable, with measurement commands and timings updated and changed by the user through Command Centre software run on a standard PC. The Command Centre software allows data to be automatically downloaded at given intervals from the measurement system. A data management scheme has been implemented that allows data to be automatically stored and catalogued in a database making it easily accessible for retrieval, processing and interpretation. Data transmission is via the TCP/IP protocol allowing the use of several existing types of remote telecommunications including GSM, PSTN, GPRS and 3G. Enhancements to the ALERT system at this site have included additional logging capability to address additional sensor types, including environmental and geotechnical sensors. The system is housed in a weatherproof enclosure and is powered by batteries charged by a wind turbine and solar panels, with back-up power supplied by a fuel cell.

Sensor network

ERT electrode arrays were permanently installed within a grid with dimensions $x = 38$ m and $y = 147.25$ m (Figure 3). Electrodes were separated by 4.75 m in the y-direction and by 9.5 m in the x-direction, and were installed in segments, each comprising 16 electrodes. This segmented design was used so that individual sections of the array are relatively easy to replace when breakage occurs due to ground movement. Each of the 16-way array segments and additional geotechnical and environmental sensors has been connected to the ALERT instrument located in the centre of the imaging area. A weather station, tilt meters, pressure transducers for pore pressure measurement, and multilevel temperature sensor arrays have been installed at the site.
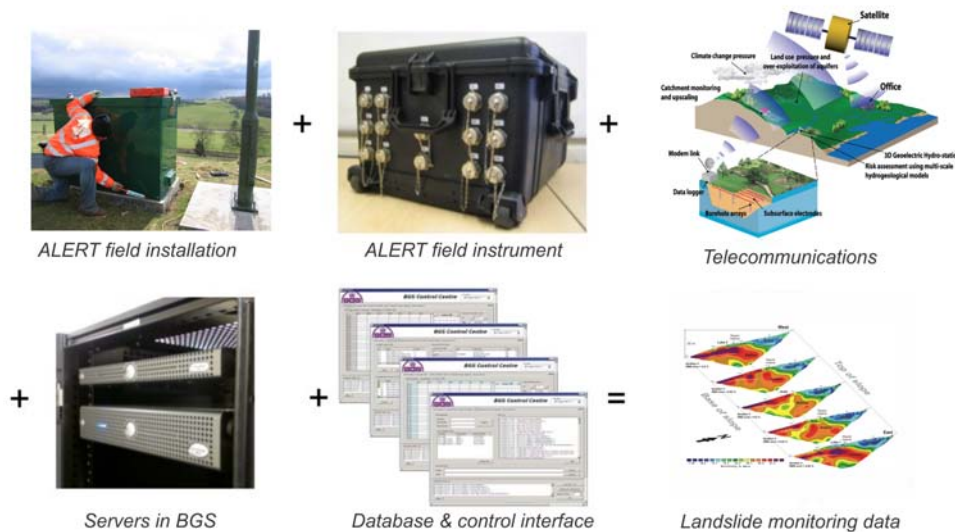
Figure 2 ALERT (Automated time-Lapse Electrical Resistivity Tomography) concept overview.

Geoelectrical data collection and inversion

The 3D ERT data sets are collected using a dipole-dipole array with dipole sizes (a) of 4.75, 9.5, 14.25, and 19 m and dipole separations (n) of 1a to 8a, and include a full set of reciprocal measurements. The data were inverted using l1-norm implementations of the regularized least-squares optimization method (Loke and Barker, 1996). The forward problem was solved using the finite-element method, in which node positions were adjusted to allow topography to be taken into account in the inversion process (Loke, 2000).

Figure 3 Site plan showing the location of the ALERT station, ERT monitoring arrays (blue lines, numbered), major geomorphologic features (top and base of the main scarp - black dashed lines; toe of the earthflows - dotted black lines) and bedrock geological boundaries (white dashed lines) between the DF, WMF, SSF, & RMF. (Aerial Photo © UKP/Getmapping Licence No. UKP2006/01).

Property Interrelationships

Field observations are being supported by laboratory testing of site materials to establish geophysical-geotechnical property interrelationships for the calibration of the time-lapse geophysical images (e.g. Cassiani et al., 2009). The aim of this testing is to establish resistivity-moisture content, and moisture content-pore pressure relationships for WMF and SSF.

Results

3D Characterisation

A 3D ERT model generated from data collected shortly after ALERT system installation is shown in Figure 4. This model serves to both reveal the 3D structure of the landslide and provide a reference model for subsequent ERT monitoring events.

The succession from low resistivity RMF, to more resistive SSF, to low resistivity WMF is clearly displayed, and is consistent with borehole results for the site (Chambers et al, 2011). The interface between the SSF and the WMF indicates a dip of ~ 5° to the north. The low surface resistivities (blue-green) of the 3D ERT model show the distribution and thickness of slipped WMF of the eastern and western lobes. Calibration using the intrusive data has allowed an improved interpretation of the extent of the landslide within the 3D ERT survey area. In this case, imaging of the buried interface between the SSF and the WMF has allowed the extent of the zones of depletion and zones of accumulation to be accurately determined.
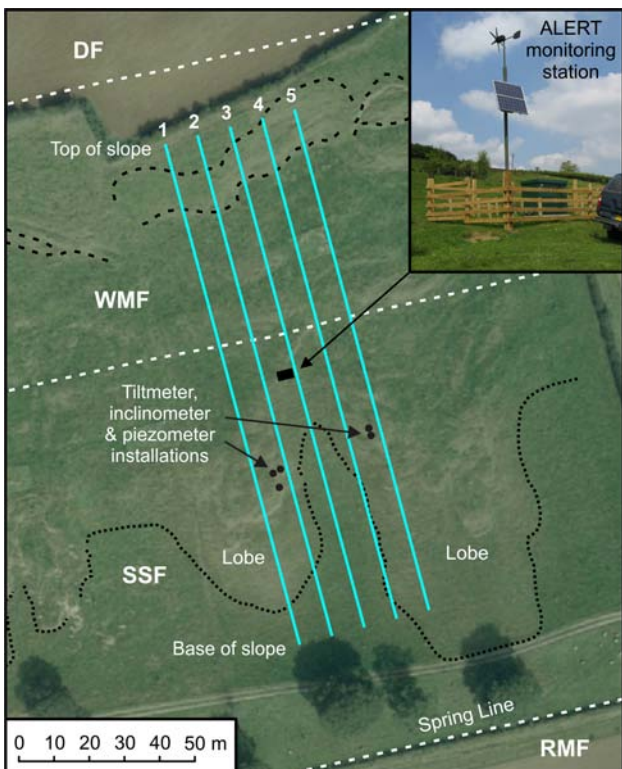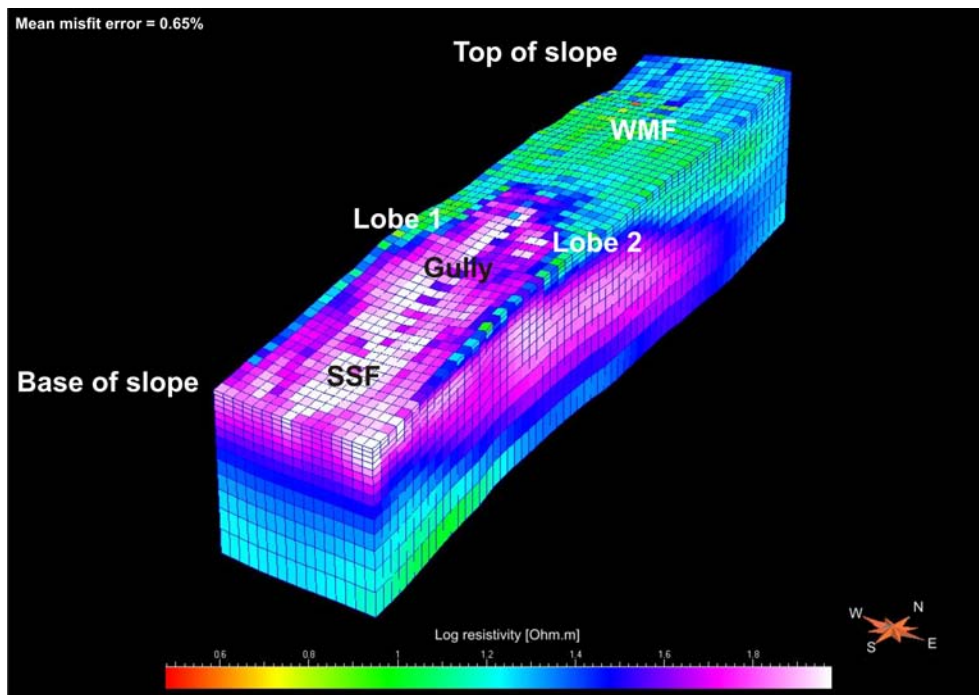
Figure 4 Baseline 3D ERT model of the landslide generated from ALERT data.

Time-Lapse Monitoring

Preliminary time-lapse images generated from the electrodes on the western boundary of the imaging area are presented in Figure 5, and include resistivity sections from August 2008 (t_1) and February 2009 (t_2), along with a difference plot showing the change during this period. These two times were chosen as they represent a dry period (t_1) and a wet period during which movement was occurring (t_2). A broad resistivity increase of ~ 20 % occurred in the top few metres (Figure 5c) between t_1 and t_2. It is likely that this is due to seasonal temperature variations, which are masking the effects of increased moisture (which would normally decrease the resistivity) during the winter. Air temperatures in the two months leading up to t_1 and t_2 were on average 16 $^{\circ}$C and 3.5 $^{\circ}$C respectively. The magnitude and extent of these apparent temperature effects are broadly consistent with those observed by Hayley et al. (2007), assuming their empirical linear approximation of ~ 2 % change in resistivity per $^{\circ}$C, with seasonal air temperature influences extending to between 5 and 10 m below ground level. Monitoring using multi-level sensors is currently being undertaken within the imaging area to determine seasonal temperature changes in the subsurface; these data will be used to correct the time-lapse ERT image for temperature effects using the methodology described by Hayley et al. (2007).

Model resistivities decreased between t_1 and t_2, below depths of 5 m, with the most pronounced decrease having occurred in the region of the model where SSF was overlain by slipped WMF. This was at a depth where temperature should be constant, and so the decrease was probably due to increased moisture content resulting from drainage of water through the disturbed WMF into the SSF during the winter months. Laboratory testing of borehole core recovered from the site is being undertaken to determine the resistivity-moisture content relationships for the WMF and SSF, which will then be used to calibrate the resistivity model.

Significant variability in model resistivity changes were seen across the top of the model between y = 35 & 75 m. Walkover surveys revealed very significant fissuring and movement in this area during the monitoring period. Very substantial increases in moisture content were also observed in this region at t_2. Variability in both the resistivity (Figure 5b) and differential models (Figure 5c) is likely to be a function of the changed subsurface structure and moisture distribution. It is also the case that the movement of electrodes, which has not yet been accounted for in the modelling, has also caused distortions in the resistivity image. Geometric corrections to account for electrode movement will be applied to future datasets using the methodology described in the following section.

Electrode movement monitoring

ERT monitoring is particularly well suited to studying landslide processes since resistivity is sensitive to changes in saturation. However, the measured potentials depend not only on the subsurface resistivity, but also on the positions of the electrodes. These are usually assumed to be known and fixed, but on an active landslide the electrodes will move over time, typically in the order of tens of cm/y in this case. If incorrect positions are used in the inversion (e.g. if the electrodes are not resurveyed after a period of movement) then artefacts will occur in the resulting image that can obscure genuine resistivity changes in the subsurface.
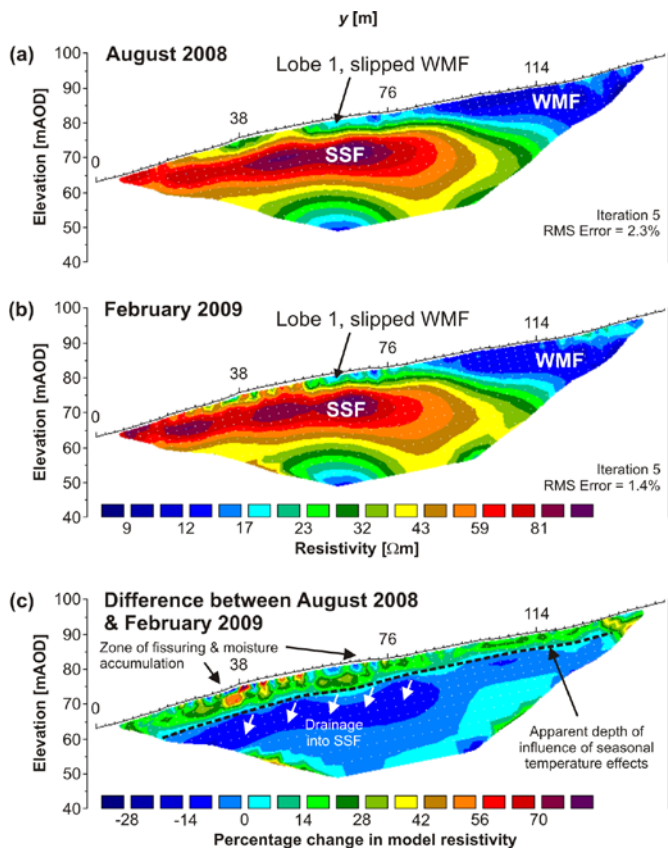
Figure 5 Time-lapse resistivity results from dipole-dipole data (a = 4.75, 9.5, 14.25 & 19 m, and n = 1 to 8) shown as 2D resistivity sections through Lobe 1. (a) August 2008 and (b) February 2009 ERT models, and (c) resulting differential resistivity image.

We have developed a method to estimate the displacements of the electrodes solely from time-lapse resistivity data (Wilkinson et al., 2010b). This has enabled us to track their movements over a complete seasonal cycle without repeated manual resurveying of their positions. Briefly the method calculates the ratio of the resistivity data at the present time to the data at a baseline time when the electrode positions were known. The ratio data are fitted to a simple model which incorporates electrode movement and layered resistivity changes consistent with those caused by seasonal temperature variations. This model is inverted to yield the estimated electrode movements from their baseline positions. The algorithm currently only works in the longitudinal direction, and does not account for small-scale resistivity changes, but we have found that the predicted movements are accurate to within 4% of the unit electrode spacing. This is sufficient to track the electrodes over time and to correct any artefacts in the resistivity images caused by using the wrong positions. An example of the predicted movements as a function of time is shown in Figure 6. The data were measured on line 1, which crosses one of the active earth flows, for just over one year and the results match the expected seasonal behaviour (no movement during the spring and summer months, but significant activity during late

autumn and winter). Our research is ongoing into combining resistivity and position inversion in a single model and incorporating lateral movement, both of which should improve the accuracy of the results.
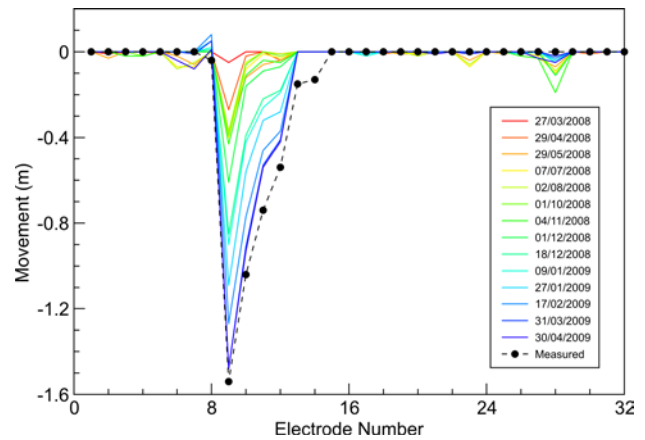

Figure 6 Predicted downslope electrode movements between March 2008 and May 2009. The measured positions in August 2009 are shown by filled circles. The electrode number increases to the north (i.e. up the slope).

Summary

A fully operational geophysical/geotechnical monitoring system has been installed on an active landslide in the UK. Initial results have demonstrated that the system can reveal 3D structure of the landslide and monitor temporal changes in the slope, including changes in moisture content and the movement of the landslide. The long-term goal is to produce calibrated 3D models of the subsurface moisture content variations from the time-lapse resistivity data. This will require petrophysical resistivity-saturation and resistivity-temperature relationships, derived from in-situ monitoring and laboratory studies.

Acknowledgments

References (in the alphabetical order)

Cassiani G, Godio A, Stocco S, Villa A, Deiana R, Frattini P, Rossi M (2009) Monitoring the hydrologic behaviour of a mountain slope via time-lapse electrical resistivity tomography. Near Surface Geophysics. 7(5-6): 475-486.

Chambers J E, Wilkinson P B, Kuras O, Ford J R, Gunn D A, Meldrum P I, Pennington C V L, Weller A L, Hobbs P R N, Ogilvy R D (2011) Three-dimensional geophysical anatomy of an active landslide in

Lias Group mudrocks, Cleveland Basin, UK. Geomorphology. 125: 472-484.

Ford, J R, in press. Geological Map of the High Stittenham Area (Sheet SE66NE). British Geological Survey, Nottingham, UK.

Hayley K, Bentley L R, Gharibi M and, Nightingale, M (2007) Low temperature dependence of electrical resistivity: Implications for near surface geophysical monitoring. Geophysical Research Letters. 34 : L18402.

Jongmans D, Garambois S (2007) Geophysical investigation of landslides: a review. Bulletin De La Societe Geologique De France. 178(2): 101-112.

Kuras O, Pritchard J D, Meldrum P I, Chambers J E, Wilkinson P B, Ogilvy R D, Wealthall G P (2009) Monitoring hydraulic processes with automated time-lapse electrical resistivity tomography (ALERT). Comptes Rendus Geoscience. 341(10-11): 868-885.

Lebourg T, Binet S, Tric E, Jomard H, El Bedoui S (2005) Geophysical survey to estimate the 3D sliding surface and the 4D evolution of the water pressure on part of a deep seated landslide. Terra Nova. 17(5): 399-406.

Loke M H, Barker R D (1996) Practical techniques for 3D resistivity surveys and data inversion. Geophysical Prospecting. 44(3): 499-523.

Loke M H (2000) Topographic Modelling in Electrical Imaging Inversion EAGE 62nd Conference and Technical Exhibition. Glasgow, Scotland.

Ogilvy R D, Meldrum P I, Kuras O, Wilkinson P B, Chambers J E, Sen M, Pulido-Bosch A, Gisbert J, Jorreto S, Frances I, Tsourlos P (2009) Automated monitoring of coastal aquifers with electrical resistivity tomography. Near Surface Geophysics. 7(5-6): 367-375.

Wilkinson P B, Meldrum P I, Kuras O, Chambers J E, Holyoake S J, Ogilvy R D (2010a) High-resolution Electrical Resistivity Tomography monitoring of a tracer test in a confined aquifer. Journal of Applied Geophysics. 70(4): 268-276.

Wilkinson P B, Chambers J E, Meldrum P I, Gunn D A, Ogilvy R D, Kuras, O (2010b) Predicting the movements of permanently installed electrodes on an active landslide using time-lapse geoelectrical resistivity data only. Geophysical Journal International. 183(2): 543-556.